Received: 15 May 2019 | Revised: 16 October 2019 | Accepted: 18 October 2019

DOI: 10.1002/bio.3733

RESEARCH ARTICLE

LUMINESCENCE The Journal of Biological and Chemical Luminescence WILEY

Nanographite-based fluorescent biosensor for detecting microRNA using duplex-specific nuclease-assisted recycling

Qizhi He[1] | Huaiqing Luo[1] | Lingli Chen[2] | Jun Dong[1] | Keke Chen[1] | Yi Ning[2]

[1]Department of Human Anatomy, Histology and Embryology, Institute of Neuroscience, Changsha Medical University, Changsha, Hunan, China

[2]Department of Microbiology, The Medicine School of Hunan University of Chinese Medicine, Changsha, Hunan, China

Correspondence
Yi Ning, Department of Microbiology, The Medicine School of Hunan University of Chinese Medicine, Changsha. Hunan, 410208, China.
Email: 15575915784@163.com

Funding information
Hunan Provincial Level Course; Key Subjects of Hunan University of Chinese Medicine; Doctor start-up Foundation of Hunan University of Chinese Medicine, Grant/Award Number: 9982-1001019; Education Department of Hunan Province, Grant/Award Number: 19C; /Natural Science Foundation of Hunan Province, Grant/Award Number: 2019JJ50693; Hunan Key Laboratory Cultivation Base of Research and Development of Novel Pharmaceutical Preparations, Grant/Award Number: 2016TP1029; National Natural Science Foundation of China, Grant/Award Numbers: 81803964, 81874375

Abstract

The development of a nanographite (NG)-based fluorescent biosensor for detecting microRNA (miRNA) is reported. Duplex-specific nuclease (DSN)-assisted signal amplification was key to its function. In the absence of a target, with the assistance of p-stacking interactions, the NG adsorbed the double carboxyfluorescein (FAM)-labelled probe (DFP) whose surface was perfectly complementary to miRNA, leading to quenching of FAM fluorescence. In the presence of a target, double-stranded DNA/RNA hybrids were repelled by the NG and fluorescence was restored. Meanwhile, the considerable increase in signal strength and sensitivity suggests DSN-mediated target recycling as an application. The detection limit of the proposed biosensor for miRNA was 10 pmol/L; there was a linear correlation when the miRNA concentration ranged from 50 pmol/L to 5 nmol/L. Additionally, the method could distinguish let-7b from most let-7 miRNA family members and was successfully used in a sample assay. This biosensor is a novel and highly sensitive tool for miRNA detection and has great potential for biochemical research, disease diagnosis, and therapy.

KEYWORDS

biosensor, enzymatic reaction, miRNA, nanographite, target recycling

1 | INTRODUCTION

MicroRNAs (miRNAs), which are characterized as endogenous and small noncoding RNAs containing approximately 19–23 nucleotides, play critical roles in various biological processes such as gene expression, protein synthesis, mammalian cell proliferation, and differentiation.[1–3] Emerging evidence suggests that the level of miRNA expression is strongly correlated with the occurrence and development of many diseases, including cancer.[4,5] miRNAs are considered ideal cancer biomarker candidates for early clinical diagnosis. Therefore, the detection of miRNAs with high sensitivity and selectivity in biological fluids is of great importance for the early diagnosis of cancers, and may also reveal novel therapeutic targets.

However, certain characteristics of miRNAs, such as their short lengths, similar sequence among family members, and low content in biological fluids, has made it challenging to develop robust detection methods. Approaches for detecting miRNAs have mainly focused on northern blotting, real-time polymerase chain reaction (RT-PCR), and microarray-based methods.[6–8] The northern blotting technique was a standard tool for miRNA analysis in early miRNA profiling studies. However, its disadvantages of low sensitivity and specificity, and that it is a time-consuming and laborious procedure, have made northern blotting unsatisfactory. Although RT-PCR can be used to optimize sensitivity and specificity, the expensive equipment requirements, and the high risk of contamination during the complex pretreatment process remain significant issues. Moreover, RT-PCR involves an essential step of reverse transcription, which

greatly increases experimental cost and design complexity. The most outstanding feature of microarray-based methods is their ability to detect multiple samples simultaneously; such methods can be used as a high-throughput test for various samples in a microarray. However, in addition to the complexity of the analytical instrumentation needed for the test, microarray technology is somewhat limited in the analysis of low-abundance transcripts; monitoring the expression of low-abundance miRNAs is highly demanding. Biosensors based on colorimetric, fluorometric, or surface plasmon resonance methods are alternative approaches for miRNA assaying.[9–11] They are superior to conventional techniques but suffer from their own limitations, including high background, the need to purchase expensive nanomaterials, and the requirement of complex electrode modification. Accordingly, new approaches are needed for the efficient detection of miRNAs.

Nanographite (NG) is a form of carbon that has attracted extensive interest in materials science, biological sensing, and targeted transport due to its unique physical, chemical, thermal, and mechanical properties.[12,13] It has an ultrahigh surface area that can be loaded with various types of molecules, including nucleic acids, proteins, liposomes, and chemical drugs, through physical adsorption or chemical coupling.[14–16] NG is considerably different from organic quenchers. Its broad absorption spectrum enables it to quench a wide range of fluorophores at a high signal-to-noise (S/N) ratio and low background via fluorescence resonance energy transfer (FRET).[17] It is relatively easier and less expensive to produce NG than single-walled carbon nanotubes and graphene oxide. NG has been used in bioimaging, drug delivery, and especially biosensor applications because of its low cytotoxicity, good biocompatibility, and storage stability. Biosensors have been created to detect heavy ions and *Salmonella enteritidis* using NG-based sensing platforms.[18,19] However, there is an absence of sensitive and selective NG-based platforms for miRNA detection.

Many enzymes, such as endonuclease, exonuclease, and DNA polymerase, have been used to enhance the sensitivity of sensing platforms for many assays.[20–22] These enzymes can induce endonuclease or polymerization reactions, leading to the target being released for the next round of reactions. Enzyme-mediated target recycling methods can significantly enhance the signal strength and sensitivity of the detection method. Duplex-specific nuclease (DSN) can readily discriminate between perfectly and imperfectly matched short duplexes, even in sequences differing by only one base. It can digest double-stranded DNA (dsDNA) or DNA in DNA/RNA hybrids, and is inactive toward single-stranded DNA (ssDNA) and single- or double-stranded RNA. Because of these features, DSN-assisted target recycling and signal amplification is highly suitable for miRNA analysis.

Here, we report a cost-effective, sensitive, and specific fluorescent biosensor for the detection of miRNA let-7b that is expressed in many cancer cells. The biosensor was based on DFP/NG conjugates and used DSN-assisted signal amplification. In the absence of a target, DFP was adsorbed onto the NG surface, whereupon the FAM fluorescence was quenched. When the target was introduced, competition from the target caused the DFP to detach from the NG surface, leading to restoration of fluorescence. Also, upon the addition of DSN, DFP was hydrolyzed, generating a large amount of FAM. Meanwhile, miRNA was released from DNA/RNA hybrids for the next cycle of reactions. The fluorescence signal became greatly amplified in this way. We used this sequence to design a rapid, sensitive, and selective bioassay for miRNA detection for use in early clinical diagnosis and treatment.

2 | EXPERIMENTAL

2.1 | Materials and reagents

NG (particle size: 5–15 nm) was obtained from Xianfeng Materials Technology (Nanjing, China). The DSN was obtained from Evrogen JSC (Moscow, Russia). The human breast cancer cell line (MCF-7), human cervical cancer cell line (HeLa), and human lung cancer cells (A549) were purchased from the Cell Resource Center of the Life Science College of Shanghai (Shanghai, China). The three healthy human serum specimens and the four cervical cancer patient serum samples were obtained from the Affiliated Hospital of Changsha Medical College (Changsha City, China). The FAM-labelled DFP and miRNA sequences were synthesized using Shanghai Sangon Biological Engineering Technology & Services (Shanghai, China) (Table S1), which also provided a total RNA (including miRNA) extraction and purification kit. All of the mother liquors and buffers used in the experiments were prepared with Milli-Q water that was subsequently treated with diethylpyrocarbonate and subjected to high-pressure steam disinfection. The other chemicals were of analytical reagent grade quality and were used as received without further purification.

2.2 | Apparatus

An LS55 luminescence spectrometer (PerkinElmer, Wokingham, UK) was used for fluorescence emission spectral analysis. Samples were placed in a quartz cuvette and measured at room temperature. Slit width was 10 nm for both excitation and emission measurements. Excitation at 495 nm caused fluorescence; intensity was measured at 520 nm. The Milli-Q water purification system had an electric resistivity of 18 MΩ·cm.

2.3 | Methods

2.3.1 | Preparation of the NG solution

NG (100 mg) was dissolved in Milli-Q water (100 ml). The mixture was ultrasonically homogenized using an ultrasonic cell disruptor in an ice bath at 150 W. After 3 h, a homogeneous NG solution (final concentration: 1 mg/ml) was obtained and stored at room temperature prior to use.

2.3.2 | Optimization of the sensing conditions

The optimal NG concentration and the optimal amount of DSN and its digestion time were determined as follows. The DFP and NG solutions were incubated in Tris–HCl buffer (25 mmol/L Tris–HCl, 5 mmol/L $MgCl_2$, pH 8.0) at room temperature before the target was introduced. Six different concentrations of NG ranging from 0 to 0.1 mg/ml were incubated with 50 nmol/L DFP at room temperature for 25 min to identify the optimal ratio of NG to DFP. Then, 5 nmol/L of miRNA let-7b was added to the NG/DFP mixtures and incubated for 25 min at room temperature. Next, 1 μl of DSN (1 U/μl) was injected into the solution. The fluorescence was monitored every 5 min as the digestion time assay. Finally, after 5 nmol/L of miRNA let-7b being added to the prepared NG/DFP complex, nine different concentrations of ExoIII ranging from 0 to 1.6 U were then added for 55 min incubation at 37°C. The volume of the reaction was always 100 μl. Fluorescence was generated by excitation at 495 nm, and the signal intensity was measured at 520 nm. The experiments were performed in triplicate.

2.3.3 | Sensitivity and selectivity assays

The DFP solution (50 nmol/L) was mixed with the NG solution (8 μl; 1 mg/ml) in Tris–HCl buffer (25 mmol/L Tris–HCl, 5 mmol/L $MgCl_2$, pH 8.0) for 25 min. Then, DSN (1 μl; 1 U/μl) and the target sequence with different concentrations ranging from 0 to 5 nmol/L were added simultaneously to the DFP/NG solution and allowed to react for another 55 min at 37°C. Fluorescence was measured at 520 nm in a quartz cuvette. Additionally, selectivity was assessed using miRNA let-7b and its family members; i.e., miRNA let-7a, miRNA let-7c, miRNA let-7d, and miRNA let-7e with two, one, four, and three base mismatches, respectively. The concentration of the target was 3 nmol/L, while that of its analogues was 6 nmol/L. The protocol was the same as that described above. All experimental procedures were performed in triplicate.

2.3.4 | Real sample analysis

The cancer cell lines MCF-7, HeLa, and A549 (approximately 10^8 cells) were chosen for this experiment. Trypsin was first used to digest the cells. Next, the treated cells were washed three times with fresh culture medium and suspended in Tris–HCl buffer. The cells were centrifuged at 17,000 *g* for 10 min at 4°C, and the sediment was collected. Then, total RNA including miRNA was extracted from the cell sediment with 1.5 ml Tris–HCl solution (10 mmol/L Tris–HCl, pH 7.4) made with RNase-free water as the solvent and quantified with a total RNA (including miRNA) extraction and purification kit. The resulting extract was used for the target miRNA let-7b assay. Additionally, different concentrations of miRNA let-7b were added to the same extract to determine the reliability of the proposed bioassay. Furthermore, three healthy human serum specimens were spiked with different concentrations of miRNA let-7b to demonstrate the feasibility of this bioassay in these serum samples. Finally, our method and quantitative RT-PCR (qRT-PCR) were compared by quantifying the expression of miRNA let-7b in four cervical cancer patient serum samples. The detection protocol was the same as previously described. The qRT-PCR data were provided by the Biological Experimental Center of Hunan Normal University. All of the experimental procedures were performed in triplicate.

3 | RESULTS AND DISCUSSION

3.1 | Principle of the sensing platform

The merits of NG and DSN were used to design a new fluorescent biosensor for a miRNA let-7b assay based on DSN-assisted target recycling and signal amplification. Figure 1 schematically illustrates this biosensor. The ssDNA probe, whose 5′- and 3′-termini were FAM-labelled, perfectly complemented miRNA let-7b. In the absence of a target, DFP binds to the surface of the NG via p-stacking interactions. The FAM dye exhibits very low fluorescence as a result of FRET. When the target is added, DFP competes with the NG and the target, leading to fluorescence restoration. The target quantum can be obtained via the increased fluorescence. Upon addition of the DSN, the DNA sequence in DNA/RNA hybrids is cleaved, thereby simultaneously releasing the target RNA and FAM fluorophores. The released RNA recycles repeatedly, resulting in the accumulation of free FAM fluorophores. This recycling process significantly enhances the sensitivity of the method, endowing it with the ability to assay analytes of low abundance in real samples.

3.2 | Feasibility analysis

The fluorescence emission spectrum of DFP under different conditions was investigated to verify the feasibility of our strategy. Figure 2 shows that the fluorescence emission of DFP in the absence of NG was much stronger (curve 1) than when NG was absent. When NG was introduced, more than 95% of the fluorescence was quenched (curve 2), which indicated that DFP had adsorbed on the NG surface, triggering FRET. The fluorescence signal did not increase when DSN alone was injected into the DFP/NG complex, which revealed that DSN was inactive toward DFP adsorbed onto NG (curve 3). Additionally, the fluorescence signal recovered following the addition of 5 nmol/L of the target (curve 4), indicating that DFP specifically bound to the target and led to the expulsion of DNA/RNA hybrids from the NG. Moreover, the fluorescence intensity was approximately 2.4-times higher when the DSN-aided endonuclease reaction occurred (curve 4 vs. curve 5). The DNA sequence harboured in the DNA:RNA hybrids was cleaved using DSN, leading to the target RNA being released for the next round of reactions and the simultaneous accumulation of free FAMs. When a single FAM-labelled probe was used for this assay, the fluorescence intensity was much lower (curve

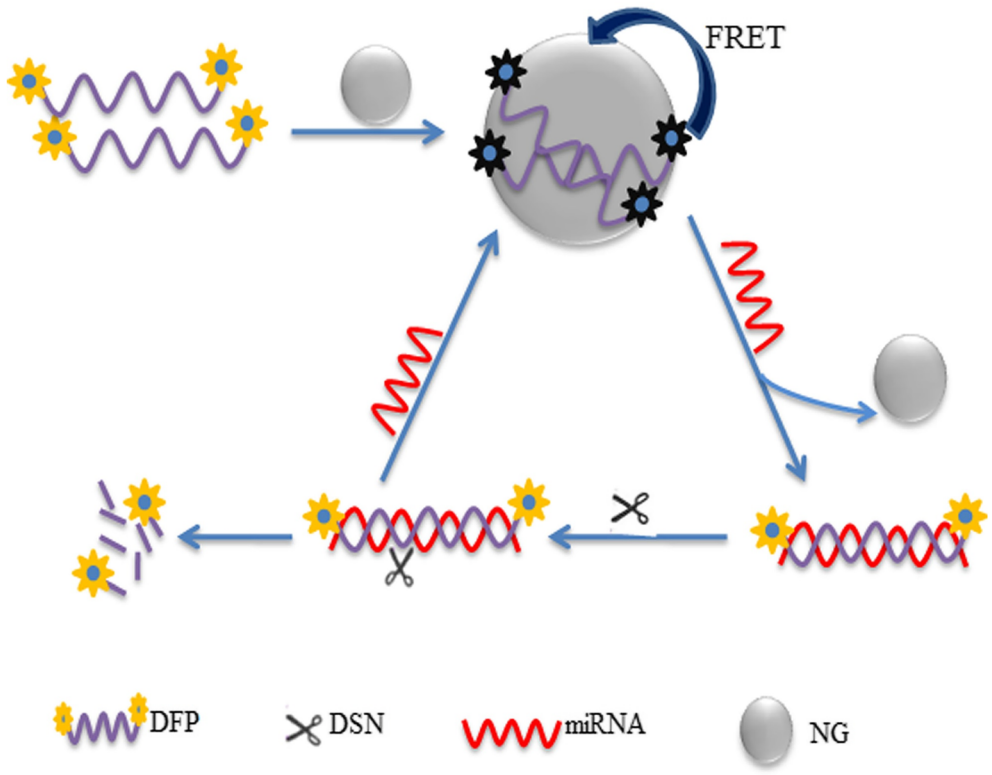

FIGURE 1 Schematic representation of the NG/DFP sensing platform for miRNA detection. In the absence of target RNA, DFP binds to NG via π-stacking and quenches the fluorescence of DFP. However, in the presence of target RNA, the probe will detached from NG due to the formation of DNA/RNA hybrids. Moreover, the signal is considerably amplified by applying DSN-assisted target recycling

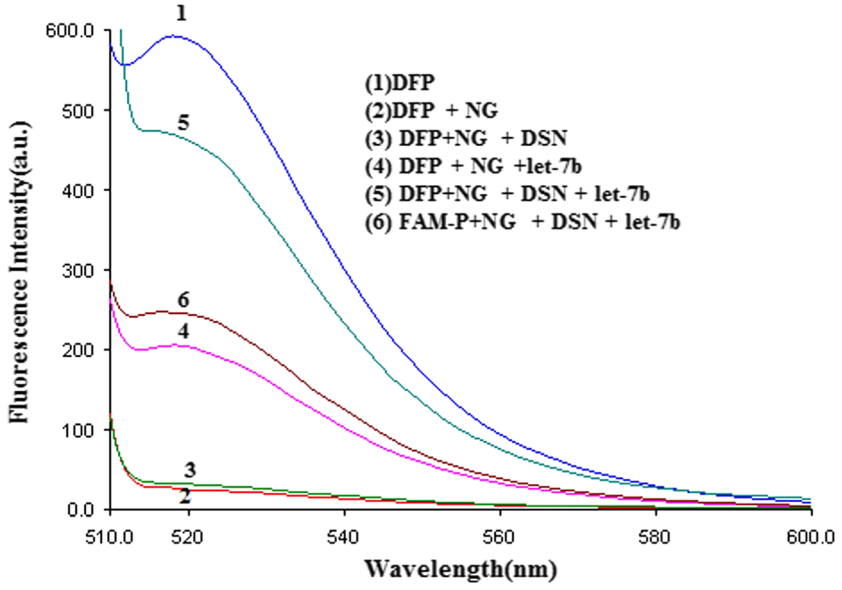

FIGURE 2 Feasibility assay. (1) DFP; (2) DFP + NG; (3) DFP + NG + DSN; (4) DFP + NG + target; (5) DFP + NG + DSN + target; (6) FAM-P + NG + DSN + target. NG concentration: 0.08 mg/ml; DFP concentration: 50 nmol/L; target concentration: 5 nmol/L; DSN concentration: 1 U. λ_{em} = 520 nm and λ_{ex} = 495 nm

6 vs. curve 5), indicating that the DFP greatly improved the fluorescence in this detection system. We therefore conclude that the bioassay is not only feasible for miRNA analysis, but also improves the sensitivity of the analytical method.

3.3 | Optimization of experimental parameters

The ratio of NG to DFP was adjusted to identify the optimal sensing performance. Figure S1(a) shows that the fluorescence gradually decreased with increasing amount of NG added to 50 nmol/L of DFP, and when the concentration of NG reached 0.08 mg/ml, more than 95% of the FAM fluorescence was quenched. Additionally, there was no change in the fluorescence when the concentration of NG exceeded 0.08 mg/ml, which revealed that the fluorescence of the 50 nmol/L FAM-labelled probe can be efficiently quenched by 0.08 mg/ml NG via energy transfer. This result reveals that the bioassay has a high S/N ratio and low background noise. Therefore, 0.08 mg/ml was selected as the optimized NG concentration. In addition, the optimal digestion time of DSN and its optimal concentration

were studied. Figure S1(b) shows that the fluorescence intensity gradually increased with increasing digestion time until 55 min. During this time, the DFP was cleaved using DSN, FAM accumulated, and the target was released from DNA/RNA hybrids for the next round of reactions. This process greatly enhanced the sensitivity of this method. Figure S1(c) displays the fluorescence variation upon the addition of different concentrations of the DSN. With the increase of DSN, the fluorescence intensity increases gradually. The fluorescence intensity shows no obvious change when concentration of DSN reaches 1 U. This demonstrate that the FAM-labelled probe was cleaved using DSN completely, leading to FAM being totally released for free. This process can yield high fluorescence and achieve good sensitivity. Therefore, the optimal digestion time of DSN and the optimal concentration of DSN are 55 min and 1 U, respectively.

3.4 | Sensitivity and selectivity of the biosensor

Different concentrations of the target, ranging from 0 to 5 nmol/L, were investigated to assess the sensitivity of the biosensor. Figure 3 shows that the fluorescence intensity increased with increasing target concentration from 0 to 5 nmol/L. The linear range was from 50 pmol/L to 5 nmol/L, which was fitted by the equation Y = 0.073X + 117.04, where Y is the fluorescence intensity and X is the target concentration (regression coefficient R^2 = 0.9985). Moreover, the detection limit of this bioassay for the target RNA was 10 pmol/L. Table 1 compares the different sensing platforms used for miRNA determination. Compared with other methods, the sensitivity of our biosensor is higher than that of some of the methods[9–11,23,24] and approaches that of certain highly sensitive methods.[25–27] Additionally, our detection system is time saving (analysis complete within 2 h), cost effective, easy to use, and does not involve the synthesis of nanomaterials or the use of expensive and complex chemical modification techniques. Our biosensor displayed excellent target detection performance with high sensitivity, offering great potential for practical applications. The selectivity of this approach was evaluated using the blank and let family members, including let-7a, let-7b (target), let-7c, let-7d, and let-7e. The blank gave the lowest fluorescence response, which indicated that all of the DFPs had absorbed onto the NG and the fluorescence was quenched (Figure 4). However, obvious recovery of fluorescence was observed upon the addition of let-7b. The signals of its family members were much weaker than that

TABLE 1 Analytical performance compared with other works for miRNA detection

Methods/materials used analytical range/LODs (mol/L) references
Colorimetric/MBs[a] 5×10^{-9}-5×10^{-7}/3.8×10^{-9} [9]
Fluorescence/CuNC[b] 5×10^{-11}–10^{-8}/1.1×10^{-11} [10]
SPR[c]/AuNPs[d] 5×10^{-11} to 5×10^{-9}/4.5×10^{-11} [11]
Fluorescence/UCNPs[e] 0–5×10^{-7}/10^{-8} [23]
Fluorescence/DNA strand 10^{-15} to 5×10^{-11}/1.04×10^{-11} [24]
Electrochemical/AuNPs[d] 10^{-14} to 5×10^{-12}/3×10^{-12} [25] Fluorescence/GQDs[f] –/10^{-14} [26]
Fluorescence/CNNS[g] 5×10^{-13} to 6×10^{-10}/10^{-13} [27]
Fluorescence/NG 5×10^{-11} to 5×10^{-9}/10^{-11} this study

[a]Magnetic beads.
[b]Copper nanoclusters.
[c]Surface plasmon resonance.
[d]Gold nanoparticles.
[e]Upconversion nanoparticles.
[f]Graphene quantum dots.
[g]Carbon nitride nanosheet.

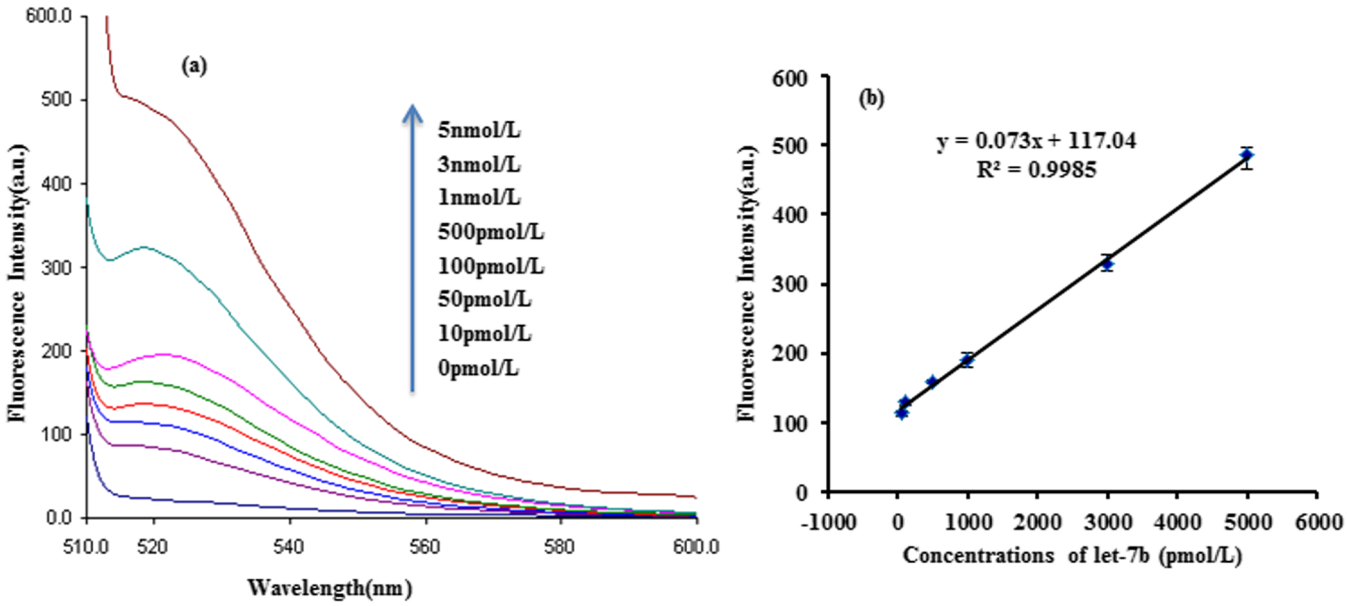

FIGURE 3 (a) Fluorescence spectra of DFP/NG in the presence of different target miRNA concentrations (from bottom to top: 0 pmol/L, 10 pmol/L, 50 pmol/L, 100 pmol/L, 500 pmol/L, 1 nmol/L, 3 nmol/L, 5 nmol/L). (b) Figure shows the relationship between the fluorescence intensity and the concentrations of target bacteria raging from 50 pmol/L to 5 nmol/L. Error bar indicates standard deviation (SD) (n = 3)

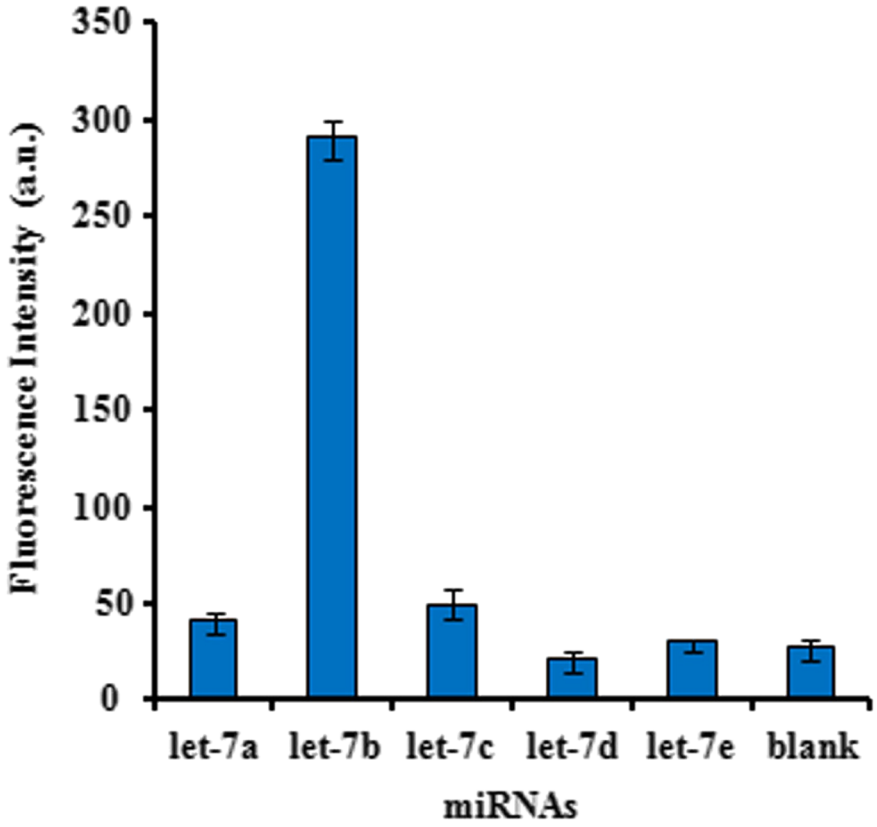

FIGURE 4 Specific detection of the target miRNA (let-7b) compared with its family members (from left to right: Let- 7a, 6 nmol/L; let-7b, 3 nmol/L; let-7c, 6 nmol/L; let-7d, 6 nmol/L; let-7a, 6 nmol/L; blank). Error bar indicates standard deviation (SD) (n = 3)

of let-7b, even when their concentrations were twice that of the target. More importantly, although the sequences of let-7b and let-7c differed by only one base, the fluorescence of the former was approximately 4.8-times greater than that of the latter. Only let-7b could induce fluorescence enhancement, and other let family members with double the concentration of let-7b failed to fluoresce. Therefore, our NG-based biosensor has high selectivity for assay of let-7b. Collectively, our method displayed excellent sensitivity and specificity for let-7b detection, which will permit its widespread use for early diagnosis and treatment of cancer.

3.5 | Analysis of miRNA let-7b in biological samples

The concentration of let-7b in extracts from MCF-7, HeLa, and A549 cells was analyzed to test the reliability of the sensing strategy in real samples. Recovery experiments were also carried out by spiking different concentrations of target let-7b into the same extracts. Table 2 shows that the let-7b content in MCF-7, HeLa, and A549 cells measured by our method was 99.91, 101.20, and 98.87 pmol/L, respectively. This indicated that our strategy could successfully discriminate the target let-7b from total RNA. Additionally, the average recoveries of MCF-7, HeLa, and A549 cells ranged from 99.28% to 100.47% with relative standard deviations (RSDs) < 2.54%, 98.52%, to 100.65% with RSD < 3.11% and 98.76% to 101.60% with RSD <3.24%, respectively (n = 3). Furthermore, different concentrations of let-7b were added to the above serum samples to determine the feasibility of the designed bioassay. Table 3 lists the recovery test results. The average recoveries ranged from 97.86% to 98.86% with RSDs < 3.09%, 98.12%, to 100.75% with RSD < 3.45% and 98.31% to 99.00% with RSD < 3.73%, respectively (n = 3). Moreover, to evaluate the accuracy of the fluorescence detection method, the expression level of let-7b in serum samples of healthy individuals (as control) and cervical cancer patients was investigated by comparing this method with qRT-PCR. Figure 5 shows that the expression level of let-7b in each of the four cervical cancer patient serum samples was higher than that in samples

TABLE 2 Analysis of let-7b in the extracted total RNA and results of recovery rates (n = 3) using the proposed bioassay

Sample	Detection result of sample (pmol/L)	Target miRNA added (pmol/L)	Found (pmol/L)	RSD (%)	Recovery (%)
MCF-7	99.91	100	198.85	1.69	99.46
		200	301.33	2.54	100.47
		300	397.05	1.96	99.28
HeLa	101.20	100	198.23	2.66	98.52
		200	303.15	3.11	100.65
		300	397.86	1.85	99.17
A549	98.87	100	202.05	3.24	101.60
		200	295.15	1.99	98.76
		300	401.98	2.80	100.78

TABLE 3 Determination of let-7b spiked with different concentrations of miRNA in human serum (n = 3) using the proposed bioassay

Sample	Target miRNA added (pmol/L)	Found (pmol/L)	RSD (%)	Recovery (%)
	100	97.86	2.12	97.86
1	200	197.32	2.55	98.66
	300	296.59	3.09	98.86
	100	98.12	2.61	98.12
2	200	201.49	3.45	100.75
	300	297.23	1.99	99.08
	100	98.31	2.54	98.31
3	200	197.47	3.28	98.74
	300	296.99	3.73	99.00

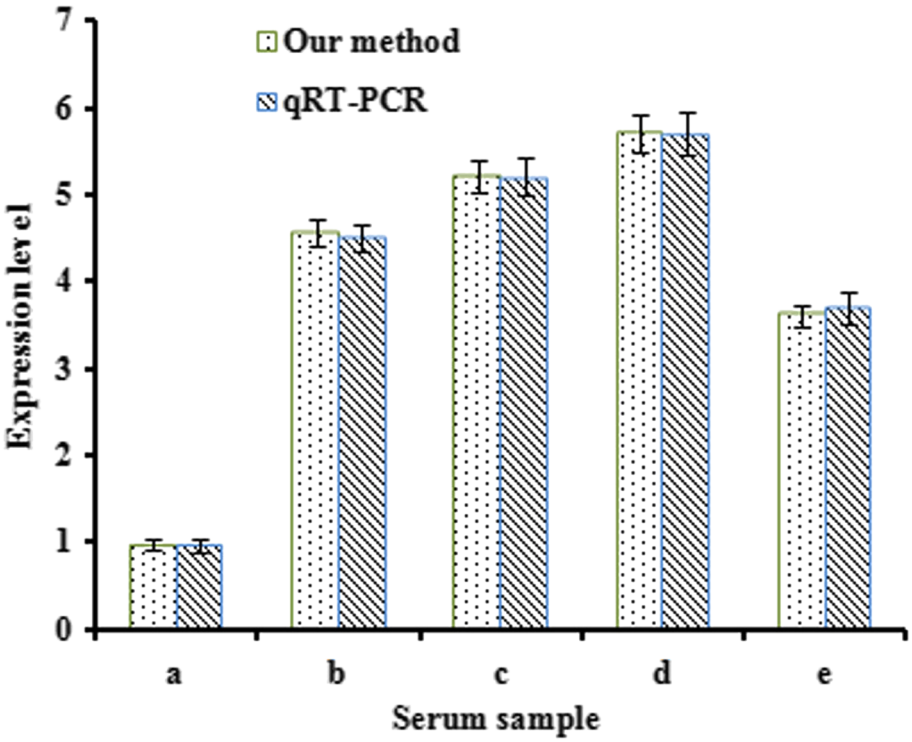

FIGURE 5 The expression level of microRNA-let 7b in different serum samples. a: Serum of healthy people. b–e: Sera from cervical cancer patients. (conditions: DFP concentration: 50 nmol/L. NG concentration: 0.08 mg/ml. DSN concentration: 1 U, time: 0–60 min). λ_{em} = 520 nm and λ_{ex} = 495 nm. Error bar indicates standard deviation (SD) (n = 3)

TABLE 4 Expression level of microRNA let7b in human serum samples (n = 3)

Samples	Detected using this method	Detected using qRT-PCR
Normal serum sample	1	1
Serum sample of cervical cancer patient 1	4.88	4.81
Serum sample of cervical cancer patient 2	5.23	5.19
Serum sample of cervical cancer patient 3	5.73	5.69
Serum sample of cervical cancer patient 4	3.65	3.69

from healthy individuals. This result is in good agreement with the outcome of the qRT-PCR method and demonstrates the accuracy of our sensing platform (the corresponding data was presented in Table 4). Collectively, these results indicate that our sensing protocol can determine target let-7b in biological samples with high sensitivity, selectivity, and accuracy.

4 | CONCLUSION

In summary, a highly sensitive and specific bioassay is successfully presented for detecting miRNA let-7b from cancer cells. It is based on NG as a quencher and DSN-aided cyclic signal amplification. This detection system has been shown to be a simple, cost-effective, time-

saving, sensitive, and selective method due to its own inherent advantages. The limit of detection (LOD) is 10 pmol/L with a good linear range from 50 pmol/L to 5 nmol/L, which is superior to many other reported sensors. In addition, the fluorescence of the experimental group compared with that of the control groups is observed when this platform is used for specific analysis, which implies that the bioassay has high specificity for miRNA let-7b. Furthermore, satisfactory results are achieved when this detection system is used for real sample analysis, which proves the potentiality of this experimental method for practical applications.

5 | FUTURE PERSPECTIVE

The system we have constructed not only provides an efficient pathway for miRNAs detection in clinical applications, but also opens up a new promising avenue for other analyte detection, such as proteins, cells, heavy ions, 16S rRNA, to name but a few. Therefore, our future study will focus on developing the kits for cancer cells and other analytes detection.

ACKNOWLEDGEMENTS

We would like to thank National Natural Science Foundation of China (81803964, 81874375), Hunan Key Laboratory Cultivation Base of Research and Development of Novel Pharmaceutical Preparations (2016TP1029), Natural Science Foundation of Hunan Province (2019JJ50693); Research Project Funded by Education Department of Hunan Province (No. 19C), Doctor start-up Foundation of Hunan University of Chinese Medicine (No. 9982-1001019), Key Subjects of Hunan University of Chinese Medicine 《pathogenic biology》 (NO.1) and Project Funded by Hunan Provincial Level Course 《Immunology and pathogenic biology》 (No. 48) for the financial support.

COMPLIANCE WITH ETHICAL STANDARDS

The authors declare that they have no conflict of interest. All procedures performed in studies involving human participants were in accordance with the ethical standards of the institutional and national research committee. This article does not contain any studies with animal performed by any of the authors. Informed consent was obtained from all individual participants included in the study.

ORCID

Yi Ning https://orcid.org/0000-0002-1097-4138

REFERENCES

[1] L. Du, T. Chen, K. Zhao, D. Yang, *Onco. Targets. Ther.* **2018**, *17*, 2195.
[2] X. Wang, Y. Song, *Biomed. Pharmacother.* **2018**, *103*, 1061.
[3] F. Duffy, E. Thompson, K. Downing, S. Suliman, H. Mayanja-kizza, W. Boom, B. Thiel, J. Weiner, S. Kaufmann, D. Dover, D. Tabb, H. Dockrell, T. Ottenhoff, G. Tromp, T. Scriba, D. Zak, *Front. Immunol.* **2018**, *13*, 1.
[4] H. Wang, R. Peng, J. Wang, Z. Qin, L. Xue, *Clin. Epigenetics* **2018**, *23*, 1.
[5] X. Liu, J. Qu, W. Xue, L. He, J. Wang, X. Xi, Y. Yin, Y. Qu, *Int. J. Chron. Obstruct. Pulmon. Dis.* **2018**, *16*, 1217.
[6] T. Tian, J. Wang, X. Zhou, *Org. Biomol. Chem.* **2015**, *13*, 2226.
[7] Y. Cheng, L. Dong, J. Zhang, Y. Zhao, Z. Li, *Analyst* **2018**, *143*, 1758.
[8] L. Moody, H. He, Y. Pan, H. Chen, *Clin. Epigenetics* **2017**, *24*, 1.
[9] X. Ji, H. Lv, M. Ma, B. Lv, C. Ding, *Microchim. Acta* **2017**, *184*, 2505.
[10] Y. S. Borghei, M. Hosseini, M. R. Ganjali, *Microchim. Acta* **2017**, *184*, 2671.
[11] K. Zeng, H. Li, Y. Peng, *Microchim. Acta* **2017**, *184*, 2637.
[12] Y. Piao, F. Liu, T. S. Seo, *ACS Appl. Mater. Interfaces* **2012**, *4*, 6785.
[13] A. N. Obraztsov, V. I. Kleshch, E. A. Smolnikova, *Beilstein J. Nanotech.* **2013**, *28*, 493.
[14] B. Pérez-López, A. Merkoçi, *Microchim. Acta* **2012**, *179*, 1.
[15] Y. Ning, Z. J. Li, Y. F. Duan, Z. H. Peng, L. Deng, *J. Nanomater Mol. Nanotechnol.* **2013**, *2*, 1.
[16] Y. F. Duan, Y. Ning, Y. Song, L. Deng, *Microchim. Acta* **2014**, *181*, 647.
[17] Z. Lu, X. Chen, Y. Wang, X. Zheng, C. M. Li, *Microchim. Acta* **2015**, *182*, 571.
[18] Y. Wei, B. Li, X. Wang, Y. Duan, *Biosens. Bioelectron.* **2014**, *15*, 276.
[19] Q. He, H. Luo, L. Tang, J. Liu, K. Chen, Q. Zhang, Y. Ning, *Microchim. Acta* **2017**, *184*, 3875.
[20] Y. Ning, K. Wei, L. Cheng, J. Hu, Q. Xiang, *Microchim. Acta* **2017**, *184*, 1847.
[21] L. Peng, Z. Zhu, Y. Chen, D. Han, W. Tan, *Biosens. Bioelectron.* **2012**, *35*, 475.
[22] Y. Ning, Q. Gao, X. Q. Zhang, K. Wei, L. L. Chen, *J. Biomol. Screen.* **2016**, *21*, 851.
[23] L. L. Mao, Z. X. Lu, N. Y. He, L. M. Zhang, Y. Deng, D. M. Duan, *Sci. China. Chem.* **2017**, *60*, 1.
[24] Y. Zhou, B. Li, M. Wang, J. Wang, H. Yin, S. Ai, *Microchim. Acta* **2017**, *184*, 4359.
[25] L. Liu, N. Xia, H. P. Liu, X. J. Kang, X. S. Liu, X. Chan, X. L. He, *Biosens. Bioelectron.* **2014**, *15*, 399.
[26] M. Laurenti, M. Paez-Perez, M. Algarra, P. Alonso-Cristobal, E. Lopez-Cabarcos, D. Mendez-Gonzalez, J. Rubio-Retama, *ACS Appl. Mater. Interfaces* **2016**, *8*, 12644.
[27] N. Fu, Y. Hu, S. Shi, S. Ren, W. Liu, S. Su, B. Zhao, L. Weng, L. Wang, *Analyst* **2018**, *143*, 1705.

SUPPORTING INFORMATION

Additional supporting information may be found online in the Supporting Information section at the end of this article.

How to cite this article: He Q, Luo H, Chen L, Dong J, Chen K, Ning Y. Nanographite-based fluorescent biosensor for detecting microRNA using duplex-specific nuclease-assisted recycling. *Luminescence*. 2019;1–8. https://doi.org/10.1002/bio.3733